A Solar Ringbom Stirling Engine

J. R. Senft

Paper No. 869112

Proceedings of the 21st

Intersociety Energy Conversion
Engineering Conference

San Diego

August 1986

UNIVERSITY OF WISCONSIN
RIVER FALLS

869112

A SOLAR RINGBOM STIRLING ENGINE

J. R. Senft

Department of Mathematics & Computer Science
University of Wisconsin-River Falls
River Falls, Wisconsin 54022

ABSTRACT

Recent work by this author demonstrated that the Ringbom Stirling engine is particularly well suited for operation at small temperature differentials. This pointed to the possibility of operating Ringbom engines from direct unfocused or from moderately concentrated solar energy. This paper describes a small low temperature differential Ringbom Stirling engine designed and constructed to test direct solar operation and collect operating data. The paper includes a discussion of scaling equations derived and used in the analytic design of the engine and details of its construction. The concept of a conical reflector used as a low power solar concentrator is introduced and the design and construction of an experimental unit is detailed. Results of the conical reflector on engine performance are presented.

A RINGBOM ENGINE is a Stirling engine with a free displacer and a crank operated piston. The gas driven free displacer gives the Ringbom several significant advantages over the conventional full kinematic Stirling. The most notable of these is the mechanical simplicity that follows from the absence of kinematic connections to the displacer. Another advantage is configurational freedom; one is free to position the displacer section in any desired orientation with respect to the piston/output drive section. A more subtle advantage of the Ringbom is the improved thermodynamic cycle that can be obtained. This is most important for low speed applications where one can design for a type of non-sinusoidal displacer motion referred to as "overdriven mode operation" [10]*. This type of operation produces a stable running engine over a large range of engine speeds. Thus Ringbom engines are a potentially important form of the Stirling for certain practical applications.

Perhaps the most important application area for Ringboms is for operation from relatively low temperature heat sources. Stirlings operating on small temperature differentials tend to have relatively low speeds and large displacer-to-piston swept volume ratios [9]. Since minimum displacer length roughly varies with the ΔT across it, low ΔT Stirlings favor large diameter displacers with short stroke. Such displacers are naturally suited to overdriven mode operation [5] and if made in flat plate form, have a natural dashpot braking effect at the ends of the displacer stroke. For these reasons Ringboms are quite well suited for low ΔT operation.

Ivo Kolin first demonstrated the possiblity of operating kinematic Stirling engines from relatively low temperature heat sources [2]. This technology was extended to Ringbom engines by the present author as reported in [9]. The displacer motion of the Ringbom proved ideally suited for low temperature differential operation with good performance over temperature differences ranging from 90°C down to 7°C.

With operation possible over this range, it was realized that these engines could operate with essentially direct solar heating or with low power concentrators not requiring continuous tracking devices. A small demonstration engine was designed, built, and used to collect data and experience under actual outdoor solar operation. This paper describes the engine, its design, and some of the results of its running trials.

DESCRIPTION OF ENGINE

Figure 1 shows the basic engine and Figure 2 is a sectional scale drawing illustrating its major features. The engine is based upon the experience gained in designing and constructing a larger engine described in [9]. Table 1 presents the primary specifications of the engine. The nomenclature used here follows that established in [10].

The engine employs a modified dashpot manufactured by the Airpot Corporation for the power piston/cylinder unit. The cylinder is precision bore Pyrex and the piston is graphitized carbon; sealing is excellent and friction is extremely low. A conventional crank/connecting rod piston drive was used with ball bearings at all pivots. A relatively large bore cylinder unit was selected to allow a short stroke to be used. With a short stroke, connecting rod angularity is small and piston side loading is minimal, so there is no need to employ a mechanism incorporating a side link [6].

The body of the displacer chamber is a plexiglas ring with a thinned wall as shown in Figure 2 to minimize thermal conduction losses. Flat aluminum endplates serve as the heater and cooler and are sealed by an O-ring fitted in the flange of the displacer chamber. The displacer body is a disc of expanded bead Styrofoam. Four triangular "windows" were cut in the disc to carry polyurethane foam regenerator elements. A drawing of the regenerative displacer is shown in Figure 3. The clearance between the displacer periphery and the chamber wall was held to the minimum obtainable within the limit of precision to which one can "machine" Styrofoam. A centering rod fitted to the hot plate together with the small Airpot displacer drive piston/cylinder establish a fixed axis for the displacer to prevent it from rubbing on the chamber wall. The regenerative displacer dramatically improves performance over a plain disc displacer with a larger annular gap flow area [13].

ENGINE DESIGN

The analytical design of the present engine was performed by scaling from the larger engine described in [9]. The larger engine was designed using the

*Numbers in brackets designate References at end of paper.

8412-0986-3/86/0869-112/$06.00/0

first order mathematical model developed in [5], [8], and [10]. The design of a Ringbom intended for low temperature differential operation is quite critical. The earlier engine performed very well over a wide range of temperature differentials. Therefore the present case was scaled from that engine in a manner that preserved, and in some respects enhanced, its operational characteristics.

A full description of the scaling equations used is presented in [12]. In the present case, the scaling held the rod-to-displacer area ratio ρ fixed. The piston-to-displacer swept volume ratio $\lambda\kappa$ was also assumed the same for similar operating temperature ratios τ. This immediately ensured that the present engine had the same common temperature ratio limit, $1 - \rho$, and, more importantly, the same critical temperature ratio limit, $\tau_c = 1 - \rho - \lambda\kappa$. From the desired piston swept volume $2 L_P A_P$ and the selected standard Airpot for the displacer drive area A_R, the displacer area A and stroke 2L were then obtained.

Two Ringboms with the same ρ, $\lambda\kappa$, and τ, and with the same dead space ratio and mean pressure, have overdriven speed limits $\bar{\omega}_1$ and $\bar{\omega}_2$ in the ratio

$$\frac{\bar{\omega}_1}{\bar{\omega}_2} = \sqrt{\frac{A_1 M_{D2} L_2}{A_2 M_{D1} L_1}} \qquad (1)$$

where M_D is displacer mass. The assumption of the same dead space ratio for both engines was quite reasonable for the present engine design. Furthermore, considering the simple case of plain displacers made of the same density material, we obtain from (1)

$$\frac{\bar{\omega}_1}{\bar{\omega}_2} = \sqrt{\frac{t_2 L_2}{t_1 L_1}} \qquad (2)$$

where t is displacer thickness.

Since solar operation was to involve ΔT values somewhat lower than the peak ΔT at which the earlier engine had been operated, a thinner displacer could be used which increased the overdriven limit as given by (2). This combined with a reduced displacer stroke, produced an overdriven speed limit increased by a factor of more than 1.5.

The piston stroke was made variable to give swept volumes ranging from 10cc to 30cc in increments of 5cc. This permits selecting a swept volume optimally matched to the temperature ratio with which the engine has to operate. The specifications given in Table 1 are based on a swept volume of 25cc, which was found best for solar operation with $T_H = 92^\circ C$ and $T_C = 27^\circ C$.

SOLAR OPERATION

For solar operation, the engine hot plate was given a layer of Thurmalox solar absorptive coating. A cover plate of 3mm thick plexiglas was fitted over the blackened hot plate with an air space of about 6mm, and the assembly sealed around the periphery. This made the hot end of the engine into a flat plate type solar collector, which is effective enough to operate the engine when tilted toward the sun.

The engine/collector makes a very interesting demonstration of unfocused solar-to-mechanical energy conversion. However, power is limited by the low temperature differentials obtained across the engine plates. Measured ΔT across the hot and cold plates was typically under $20^\circ C$ during summer operation in River Falls, Wisconsin. In an effort to further investigate the potential of this type of engine for practical applications, modifications were made to increase the ΔT across the engine.

The most obviously needed improvement was to the cooler plate. The original plate was simply a flat disc presenting an external area of about 176 cm^2. A new cooler was fabricated from a length of extruded finned aluminum. The pattern selected was flat on one side to form the heat exchanger surface within the engine. The other side carried deep fins widely separated for good convective air flow. The new cooler presented an external surface area of about 1640 cm^2. This cooler proved to be very effective in improving performance, about doubling the power output. Its contribution will be described in more detail below.

CONICAL REFLECTOR CONCEPT

One of the obstacles to small scale solar-to-mechanical conversion is the complexity of a concentrator and tracking system. This complexity translates into high capital cost and loss of portability and adaptability to a variety of tasks, both of which run contrary to the need in developing and rural areas for small versatile mechanical power sources. Indeed, this was the principal motivation for investigating low ΔT solar Stirlings. Therefore, when considering means to increase T_H, any scheme involving a high cost concentrator or a continuous tracking device was immediately ruled out. A conical reflector, since it does not focus to a point, or to a line, but rather to a relatively large area, does not require great precision in its manufacture, and does not require continuous tracking. The reflector can be inexpensively roll-formed from flat sheet material, and manual adjustment of the reflector position every hour or two is sufficient to keep the unit working at near full capacity.

The geometrical parameters of the conical reflector are shown in Figure 4: r = radius of absorption plate, R = radius of cone opening, S = slant height of cone frustum, H = axial height of cone frustum, ϕ = cone angle (included), and β = angle of incidence between reflected ray and absorption plate. As Figure 4 suggests, we restrict attention to reflectors with the property that every ray entering parallel to the axis and striking the cone reflects directly onto the absorber plate. This restriction to once-reflecting cones is a natural one. It keeps cone length down, minimizes reflection losses, and is most forgiving of aiming errors. Note that $0 < \phi < \pi/2$.

From trigonometry, a cone is once-reflecting if and only if

$$S \leq 2 r \cos\phi \csc(\phi/2) \qquad (3)$$

If equality holds in (3), the reflector will be referred to as a <u>once-reflecting full conical reflector</u>. Let I represent the direct solar flux intensity and E the total energy received by the absorber plate in the form of heat. Then for rays entering parallel to the cone axis,

$$E = a I \pi r^2 + b I \pi (R^2 - r^2) \qquad (4)$$

where $0 < a,b < 1$ are factors representing the performance of the two avenues of energy collection of the conical system. The first term of (4) arises from solar energy directly falling upon the central collector, and the factor a represents the fraction of this energy actually accepted by the plate. It

depends upon the transmissivity of the collector cover (plexiglass) and the absorptivity of the blackened receiving surface. The second term of (4) is due to the solar energy reflected from the cone onto the central collector. The factor b is the product of the reflectivity of the conical surface and the combined transmissivity and absorptivity of the central collector. Because reflected rays approach the collector at a non-normal angle β, the factor b is a function of the cone angle ϕ and $b \leq a$.

For a once-reflecting full conical reflector, $R = r(1 + 2\cos\phi)$, so equation (4) can be written as

$$E = I \pi r^2 [a + 4b \cos\phi (1 + \cos\phi)] \qquad (5)$$

It is interesting to note the performance limits of once-reflecting cones that equation (5) implies. In the ideal case, $a = b = 1$, and equation (5) yields the interesting fact that the concentration factor $C = E/I\pi r^2$ has a limiting value of 9 as vertex angle approaches zero. Of course as the concentration factor nears 9, cone length increases without bound but ideal concentration factors of up to 7 can be obtained with cones of quite practical length-to-diameter ratios. Higher concentration factors can be obtained with multiply-reflecting cones [1], but length-to-diameter ratio and sensitivity to orientation relative to incident sunlight increases.

TEST REFLECTOR

For this project a 60° conical reflector was fitted to the engine as pictured in Figure 5, and gave good results. The 60° once-reflecting cone has an ideal concentration factor of 4. To obtain an estimate of its actual performance, equation (5) with $\phi = 60°$ gives

$$E = I \pi r^2 [a + 3b].$$

Assuming the cover of the central collector has a transmissivity of .92, and the absorber surface effectiveness is .95, the factor a is about .87. Taking the total reflectivity of the cone to be .75, and the transmissivity of the collector cover to be reduced at the incidence angle of 30° by the factor .90 [4], we estimate b to be .59. Hence for the full 60° cone we obtain

$$E = 2.64\, I \pi r^2$$

This represents a concentration factor of 3 over the flat plate collector alone, with the same transmissivity and absorber surface effectiveness. The conical reflector therefore makes a considerable improvement, even after allowing for real losses.

The above calculations are based upon the axis of the cone pointing exactly at the sun. In order to assess the effects of aiming error, the results in [1] were extended by Leake [3]. Table 2 shows the concentration factor of a once-reflecting 60° full cone as a function of ray entry angle α (measured to the cone axis) and the coefficient of reflection ε of the surface of the cone. The total energy directed to the flat plate collector of the engine is then the product of the solar flux intensity, the absorber plate area, the concentration factor in the table, and the cosine of the entry angle (acceptance losses of the flat plate collector have not been included in the calculation of the concentration factors). As can be seen, performance does not rapidly decrease with pointing error. With judicious aiming, the unit will perform above 85% of peak for an hour, and above 70% of peak for two hours. Hence, the cone is quite practical for many applications without a continuous tracking device.

The 60° test cone for this project was fabricated from heavy tag board covered with 3M Brand ECP-244 solar collection film. This is an adhesive backed 0.10 mm acrylic film with a claimed reflectivity of .86 (we used a conservative .75 in the above calculation to allow for local geometric inaccuracies in the reflector surface and degradation by dust, scratches, etc.). Two rings were fastened to the outside of the cone to maintain circularity and rigidity.

RESULTS

The reflector worked very well, typically producing hot plate temperatures of 93°C. Table 3 summarizes the results of the reflector and cooler improvements made during this project. Four different collector/cooler configurations are represented ranging from the original flat plate collector and flat plate cooler (configuration #1) to the 60° conical reflector with the finned cooler (configuration #4). T_H and T_C are typical recorded hot and cold plate temperatures, and T_A is the corresponding outside air temperature. The table also lists the temperature factor F

$$F = (T_H - T_C)/(T_H + T_C)$$

and the swept volume ΔV at which the engine was operating when the corresponding temperatures were recorded. These parameters appear in the Stirling Engine Power Formula

$$P = 2\, E\, f\, \bar{p}\, \Delta V\, F$$

where P = shaft power, E = efficiency factor, $\bar{p}$ = mean cycle pressure, and f = engine frequency. This formula is derived in [5]. From the table, the increase in F and ΔV show that the addition of the finned cooler and conical reflector increased engine power by a factor of about 7.

Engine power was measured in the laboratory in order to maintain steady state conditions. Details can be found in [11]. A typical power/speed curve is shown in Figure 6. Peak power was 0.252 Watt at 270 rpm. The engine was operating on air at atmospheric pressure with ΔV = 25cc. The resulting generalized Beale number is .26.

ACKNOWLEDGEMENT

The author is grateful to the Charles A. Lindbergh Fund for a grant which made the work reported here possible.

REFERENCES

1. Burkhard, D. G., Shealy, D. L., & Storbel, G. L. "Comparison of the solar concentrating properties of truncated hexagonal, pyramidal, and circular cones" Optics Applied to Solar Energy Conversion, Vol. 114, 1977, pp 67-94.

2. Kolin, I. Isothermal Stirling Cycle Engine University of Zagreb, 1983.

3. Leake, D., Private communication, University of Wisconsin- River Falls, 1986.

4. Meinel, A. B. & Meinel, M. P. Applied Solar Energy Addison-Wesley, Reading, 1976.

5. Senft, J. R. "The hybrid Stirling engine" Proc. 16th IECEC Paper #819785, 1981.

6. Senft, J. R. "Small stationary Stirling engine design" Proc. Institute of Mechanical Engineers, Paper C19/82, University of Reading, U.K., 1982.

7. Senft, J. R. "A simple derivation of the generalized Beale number" Proc. 17th IECEC, Paper #829273, 1982.

8. Senft, J. R. "First order analysis of Ringbom engine operation" Proc. 18th IECEC, Paper #839125, 1983.

9. Senft, J. R. "A low temperature difference Ringbom Stirling demonstration engine" Proc. 19th IECEC, Paper #849126, 1984.

10. Senft, J. R. "A mathematical model for Ringbom engine operation" AMSE Journal of Engineering for Gas Turbines & Power, Vol. 107, p 590-595, July, 1985.

11. Senft, J. R. "Investigation of the potential of a direct solar Stirling engine" Final Report to the Charles A. Lindbergh Fund, Jan., 1986.

12. Senft, J. R. "Ringbom engine design" Proc. 3rd International Stirling Engine Conference Rome, 1986.

13. Stirling Engine Newsletter, August, 1985, page 2.

TABLES

A = displacer area = 132 cm^2

A_P = piston area = 8.31 cm^2

A_R = displacer rod area = .713 cm^2

L = displacer amplitude = 1/2 displacer stroke = .523 cm

L_P = piston amplitude = 1/2 piston stroke = 1.50 cm

V_D = dead volume = 14.5 cc

M_D = displacer mass = 6.0 g

Table 1. Specifications of the solar Ringbom engine.

ε \ α	0°	5°	10°	15°	20°	25°
1.00	4.00	3.62	3.23	2.85	2.46	2.06
.95	3.85	3.48	3.12	2.76	2.39	2.01
.90	3.70	3.35	3.01	2.67	2.32	1.96
.85	3.55	3.22	2.90	2.57	2.24	1.90
.80	3.40	3.09	2.79	2.48	2.17	1.85
.75	3.25	2.95	2.67	2.39	2.10	1.80

Table 2. Concentration factor as a function of ray entry angle α from cone axis for once-reflecting full 60° cone with reflection coefficient ε.

Engine Configuration	T_H	T_C	T_A	F	ΔV
1. Flat Plate Collector Flat Plate Cooler	57°C	41°C	--	.026	15cc
2. Flat Plate Collector Flat Plate Cooler	53	24	21	.046	28
3. 60° Conical Reflector Flat Plate Cooler	92	40	28	.076	25
4. 60° Conical Reflector Finned Cooler	92	27	21	.099	25

Table 3. Summary of results of collector and cooler improvements.

ILLUSTRATIONS

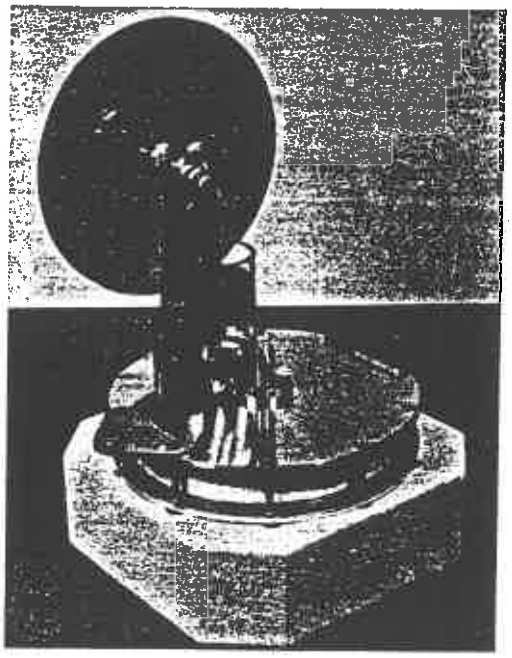

Fig. 1. Photo of the basic engine.

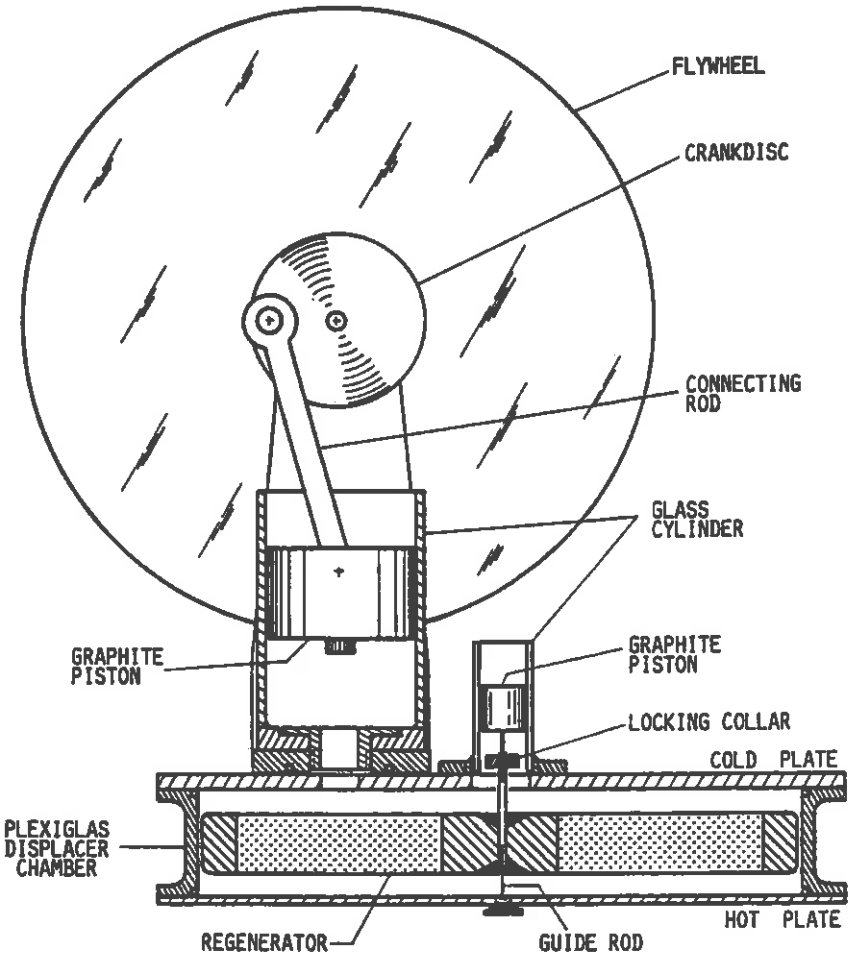

Fig. 2. Sectional drawing of engine.

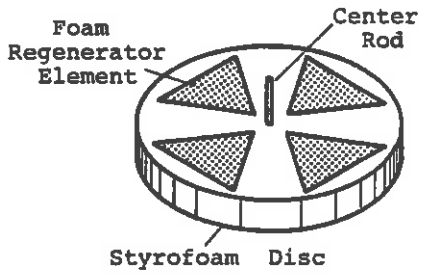

Fig. 3. The regenerative displacer.

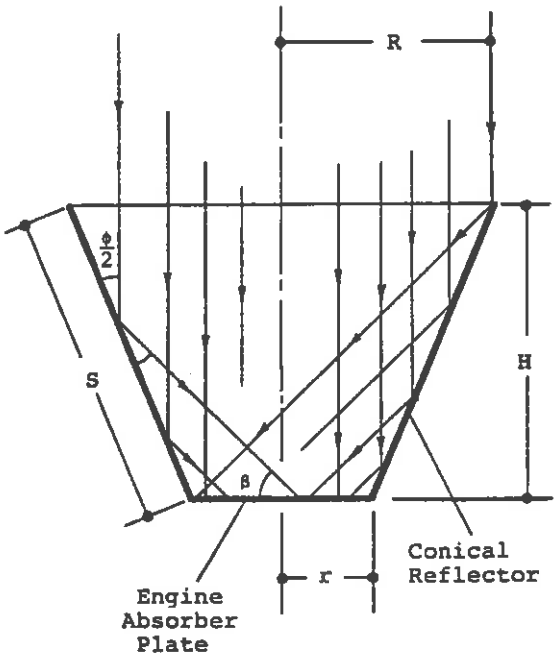

Fig. 4. Conical reflector geometry.

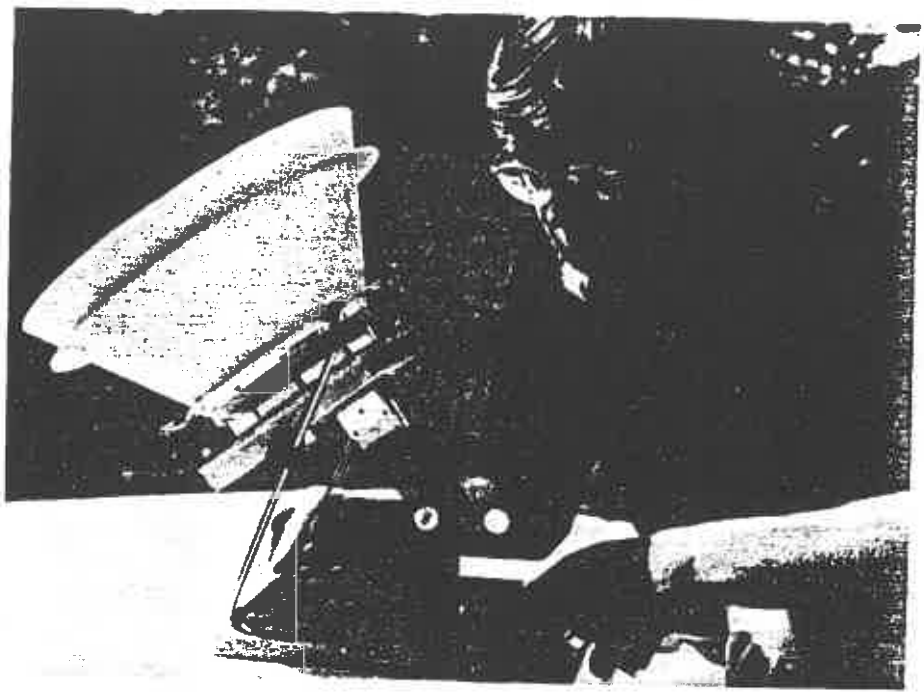

Fig. 5. The Ringbom engine with a 60° conical reflector.

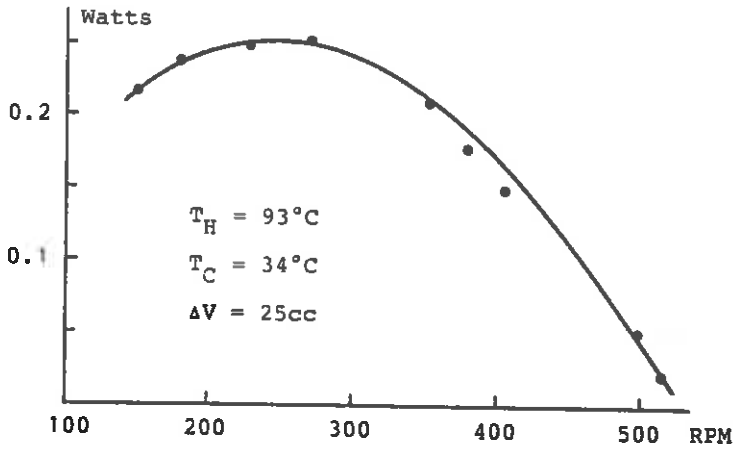

Fig. 6. Power vs. Speed curve for the engine.